Towards Real-Time 3D US to CT Bone Image Registration Using Phase and Curvature Feature Based GMM Matching*

Anna Brounstein[1], Ilker Hacihaliloglu[1] Pierre Guy[2], Antony Hodgson[3], and Rafeef Abugharbieh[1]

[1] Department of Electrical and Computer Engineering
[2] Department of Orthopaedics
[3] Department of Mechanical Engineering, University of British Columbia, Vancouver, B.C., Canada
{abrou,ilkerh,rafeef}@ece.ubc.ca, pierre.guy@ubc.ca, ahodgson@mech.ubc.ca

Abstract. In order to use pre-operatively acquired computed tomography (CT) scans to guide surgical tool movements in orthopaedic surgery, the CT scan must first be registered to the patient's anatomy. Three-dimensional (3D) ultrasound (US) could potentially be used for this purpose if the registration process could be made sufficiently automatic, fast and accurate, but existing methods have difficulties meeting one or more of these criteria. We propose a near-real-time US-to-CT registration method that matches point clouds extracted from local phase images with points selected in part on the basis of local curvature. The point clouds are represented as Gaussian Mixture Models (GMM) and registration is achieved by minimizing the statistical dissimilarity between the GMMs using an L2 distance metric. We present quantitative and qualitative results on both phantom and clinical pelvis data and show a mean registration time of 2.11 s with a mean accuracy of 0.49 mm.

Keywords: US-CT registration, point cloud matching, local phase features, curvature, Gaussian mixture model registration.

1 Introduction

US has emerged as a desirable intra-operative imaging modality for computer-assisted orthopaedic surgeries, as it is inexpensive, safe and real-time. Despite its many desirable characteristics, it can be difficult for a surgeon to utilize, since B-Mode US images are susceptible to noise, artifacts and a limited field of view. To overcome these deficiencies, US can theoretically be fused with a high resolution image that has a high signal-to-noise ratio, such as pre-operative CT, but in order for US and CT to be successfully used in tandem to visualize bone in orthopaedic surgery, they must be quickly and accurately registered.

Several methods of registering US to CT have been proposed in recent years, but current methods are not sufficiently fast for real-time use. The most widely

* This work was supported in part by NSERC and the Institute for Computing, Information and Cognitive Systems (ICICS) at UBC.

G. Fichtinger, A. Martel, and T. Peters (Eds.): MICCAI 2011, Part I, LNCS 6891, pp. 235–242, 2011.

used registration method in computer assisted orthopaedic systems (CAOS) to date is the iterative closest point (ICP) algorithm. Methods have been proposed to improve the robustness and speed of the standard ICP method [1,2]. Although relatively successful, ICP exhibits susceptibility to converging to local minima and, therefore, a close initial manual alignment is necessary. Moghari et al. [3] proposed a point-based registration algorithm based on the Unscented Kalman Filter where he achieved more robust and accurate registration results compared to standard ICP. The main drawback of their approach is the need to manually extract bone surfaces from US data. Some researchers have tried to automate the extraction of bone surfaces from US images [4]; however, the techniques were limited to two dimensions (2D). Winter et al. [5] maximized the sum of the overlapping gray values of pre-processed CT bone surfaces and the Three-dimensional (3D) US volume. While this method showed accurate registration results, it assumed a fixed probe orientation for CT pre-processing, which significantly reduces its practicality in real life applications (e.g., in fracture surgery where the US probe needs to be realigned after a fracture reduction). Penney et al. [6] created probability images of the CT and US data and registered these using a normalized cross-correlation metric. The registration results were accurate; however manual segmentation of the CT and US volumes was required to create training sets for the probability images. A more recent method for intensity-based registration involves simulating US images from re-sliced CT data [7] that is updated throughout the registration process, which Gill et al. [8] later extended for registering bone surfaces of the spine. They were able to achieve a mean target registration accuracy of 1.44 mm for phantom scans and 1.25 mm for sheep cadaver scans; however their intensity-based registration took an average of 14 minutes on a central processing unit (CPU) and 11 seconds when implemented on a graphics processing unit (GPU).

To move closer to the goal of fully automated real-time registration of 3D US to CT volumes, we propose in this paper a registration method based on using local phase information to identify surface points in the US volume, culling the points in both the US and CT volumes based in part on curvature metrics and registering the two point clouds using a GMM technique. We demonstrate improved accuracy and run-time compared to state-of-the-art techniques on pelvic phantom and clinical data.

2 Methods

2.1 Image Pre-processing and Bone Surface Extraction

One of the main challenges of point-based registration of US and CT volumes is extracting a point set from the US data that corresponds with a point set from the CT set. Recently, 3D local phase information has been proposed to extract the surfaces of bones in US volumes [9] using a 3D Log-Gabor filter, $LG(\omega)$ to extract local phase information in the B-Mode US volume:

$$LG(\omega) = e^{-\frac{log(\omega/\omega_o)^2}{2log(\kappa/\omega_o)^2}} \times e^{-\frac{\alpha(\phi_i,\theta_i)^2}{2\sigma_\alpha^2}}. \quad (1)$$

In Equation 1, κ defines the bandwidth of the filter, which determines the frequency specificity. $\alpha(\phi_i, \theta_i)$ is the filter's angle between the azimuth (ϕ) and the elevation (θ) angles. The angular bandwidth is determined by σ. The Log-Gabor filter is built on multiples of the minimum wavelength, λ_{min}, which determine the centre frequency ω_o as $\omega_o = 2/\lambda_{min} \times (\delta)^{m-1}$ for the scaling factor δ and multiple m. The even and odd components, $e_{rm}(x, y, z)$ and $o_{rm}(x, y, z)$, of $LG(\omega)$ are calculated using the real and imaginary responses of the Log-Gabor filter for each point (x, y, z). The 3D phase symmetry (PS) is defined in Equation 2 for each scale (m) and orientation (r):

$$PS_{3D}(x, y, z) = \frac{\sum_r \sum_m \lfloor [|e_{rm}(x, y, z)| - |o_{rm}(x, y, z)|] - T_r \rfloor}{\sum_r \sum_m \sqrt{e_{rm}^2(x, y, z) - o_{rm}^2(x, y, z)} + \epsilon}. \quad (2)$$

Here, T_r is a threshold to account for noise in the US image and ϵ is a small number to avoid division by zero. The bone surface is determined as the maximum PS value along the direction of the US probe.

Compared to the bone surface segmentation of US, CT segmentation is relatively simple. Typically, CT can be segmented using a binary threshold at 200 H.U. Ray-casting is then used to find the bone surface in these binary CT volumes resulting in extracted surfaces that are one voxel thick.

2.2 Point Cloud Selection and Curvature Features

After the bone surface has been extracted from both the US and the CT data, point clouds are created. Our experiments indicate that using between 800 and 1,000 points in each data set produces a reasonable trade-off between a fast run-time and accurate results when matching the volumes using GMMs. Our extraction of both US and CT bone surfaces in Section 2.1 constitutes data reduction from a volume of over 4 million voxels to approximately 10 thousand surface points. To register these volumes in real-time, it is helpful to further significantly reduce the number of points. Therefore, we sub-sample the points extracted in 2.1 to create point clouds for registration, keeping only 5% of the surface points. Though sub-sampling generally preserves the low curvature regions, high curvature regions may be significantly degraded. For example, when matching the iliac spine region of the pelvis using only a sub-sample of the bone surface, registration is accurate and robust with respect to the pelvic table. This is sufficient for 2D registration of the pelvis, but there is little low curvature variability between slices along the iliac spine and this lack of distinguishable features renders the volumes prone to mis-alignment along the crest in 3D registration. To better preserve these salient regions, we use Gaussian curvature, K, to localize high curvature features of the bone surface. K is the product of the principle curvatures κ_1 and κ_2 and is expressed as [10]: $K = \kappa_1\kappa_2 = \frac{eg-f^2}{EG-F^2}$, where $E = ||\mathbf{x}_u||^2$, $F = \mathbf{x}_u \cdot \mathbf{x}_v$ and $G = ||\mathbf{x}_v||^2$ are the coefficients of the first fundamental form, and $e = {}^{(\mathbf{x}_{uu}\mathbf{x}_u\mathbf{x}_v)}/\sqrt{EG-F^2}$, $f = {}^{(\mathbf{x}_{uv}\mathbf{x}_u\mathbf{x}_v)}/\sqrt{EG-F^2}$ and

$g = {}^{(\mathbf{x}_{vv}\mathbf{x}_u\mathbf{x}_v)}/_{\sqrt{EG-F^2}}$ are the coefficients of the second fundamental form for the surface $\mathbf{x}(u, v)$. The top decile of curvature values contribute to the point cloud.

2.3 GMM Registration of US and CT

We registered the US and CT volumes by representing the corresponding point clouds as GMMs and minimizing the distance between the models. GMMs are statistical models representing an entire population using multi-dimensional Gaussian distributions to describe sub-populations, known as components and are represent by the probability density function, $p(\mathbf{x})$. Each component density, ϕ_i, is characterized by its mean, μ_i and its covariance matrix, Σ_i. Using a GMM to represent a point cloud alleviates the need to find point-to-point correspondence between volumes—a major obstacle in many point-based registration methods.

The GMMs are iteratively registered using the L2 similarity metric. The L2 distance has the advantage of having a closed-form solution. The registration algorithm minimizes the L2 cost function of the two GMMs representing the model point cloud, $\mathcal{M}(\mathbf{x}) = p_m(\mathbf{x})$, and the scene, $\mathcal{S}(\mathbf{x}) = p_s(\mathbf{x})$ with a rigid transformation, $\mathbf{T}(\mathcal{M}(\mathbf{x}), \theta, t)$, giving the L2 distance:

$$d_{L2}(\mathcal{M}(\mathbf{x}), \mathcal{S}(\mathbf{x}), \theta, t) = \int (\mathcal{S}(\mathbf{x}) - \mathbf{T}(\mathcal{M}(\mathbf{x}), \theta, t))^2 \mathrm{d}x. \tag{3}$$

It should be noted that the scene model, $\mathcal{S}(\mathbf{x})$, is fixed during the optimization and $\int \mathbf{T}(\mathcal{M}(\mathbf{x}), \theta, t)^2 \mathrm{d}x$ is invariant for rigid transformations, so minimizing the L2 distance in Equation 3 becomes equivalent to solving:

$$\underset{\theta,t}{\operatorname{argmin}} \left[d_{L2}(\mathcal{M}(\mathbf{x}), \mathcal{S}(\mathbf{x}), \theta, t) \right] = \underset{\theta,t}{\operatorname{argmin}} \left[- \int \mathcal{S}(\mathbf{x}) \mathbf{T}(\mathcal{M}(\mathbf{x}), \theta, t) \mathrm{d}x \right]. \tag{4}$$

Given Equation 4 and the formula $\int \phi(\mathbf{x}|\mu_1, \Sigma_1)\phi(\mathbf{x}|\mu_2, \Sigma_2)\mathrm{d}x = \phi(0|\mu_1 - \mu_2, \Sigma_1 + \Sigma_2)$, the closed form expression for the L2 distance between GMMs can be found [11].

2.4 Validation Setup

Phantom Data: In the phantom study we used a Sawbone pelvis #1301 (Pacific Research Laboratories, Inc., Vashon, WA) with 38 1 mm fiducials attached to the surface of the iliac crest and pubic bone. Ten 3D US volumes were acquired of the phantom and were used to create ten US-CT registrations. The US volumes were taken with a G.E. Volusion 730 Expert Ultrasound Machine (GE Healthcare, Waukesha, WI) using a 3D RSP4-12 probe in a water bath. The US phantom volumes were 152x198x148 voxels with an isometric resolution of 0.24 mm. A CT volume was taken with a Toshiba Aquilion 64 (Tustin, CA) and has a resolution of 0.76 mm×0.76 mm×0.3 mm. The pre-processing steps were implemented in

Matlab and the registration was implemented in C++ on a 3.0 GHz Dual Core Intel Xeon CPU using 64-bit Windows 7 and 8 GB of RAM.

Point clouds were created both with and without high curvature features. The fiducial registration error (FRE) was calculated as the average distance between all corresponding fiducial pairs found in both volumes and the surface registration error (SRE) was calculated as the rms distance between the surfaces found in the two imaging modalities.

Each of the ten data sets used for registration as described in Section 2 was comprised of one 3D US volume and a CT volume cropped to the area of interest. The phantom volumes were typically misaligned by as much as 26 degrees and translated by 22mm. For each volume, approximately 800-1000 points were automatically selected on the bone surface. Successful registration should have an error less than 2 - 4 mm for fracture reduction applications in CAOS[12].

Clinical Data: Validation was completed on three US - CT sets acquired from a pelvic fracture patient prior to fracture reduction surgery. The US volumes were acquired using the same setup as described in the phantom study. The CT volume was 512x512x121 voxels and had a resolution of 0.73 mm×0.73 mm×2.0 mm. The SRE and registration run-time were used to quantitatively validate the results.

3 Results and Discussion

Figure 1 shows the results of the pre-processing and registration of the phantom. The resulting surfaces are closely matched, as reflected by the qualitative

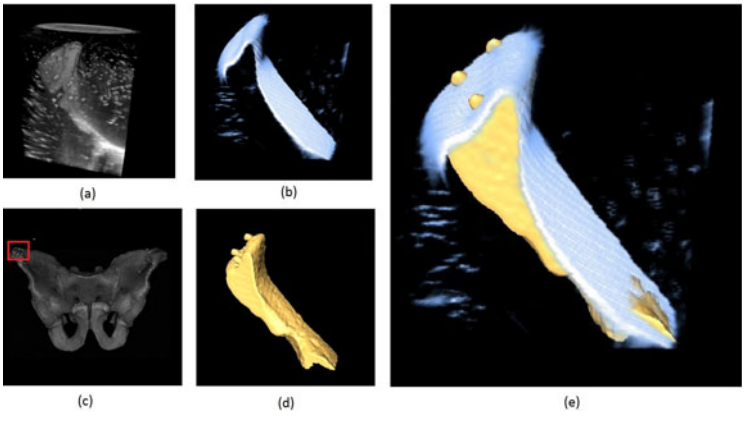

Fig. 1. Qualitative results of the phantom study: (a) is the B-Mode volume of the iliac spine. (b) is the corresponding PS volume. (c) shows the entire CT of the pelvis with the region of interest enclosed in the red box. (d) is the thresholded CT region of interest of the iliac spine. (e) shows the PS volume overlaid on the thresholded CT. Note that the fiducials are visible in both the US and CT volumes.

Phantom	K		no K	
	SRE	FRE	SRE	FRE
Mean (mm)	0.49	1.22	1.30	3.71
Median (mm)	0.42	1.24	0.80	2.10
Std. Dev. (mm)	0.30	0.45	1.26	2.98
Mean Time (s)	2.11		2.12	

(a)

Clinical Scans	K	no$K$
Mean (mm) SRE	0.63	0.84
Mean Time (s)	1.99	1.75

(b)

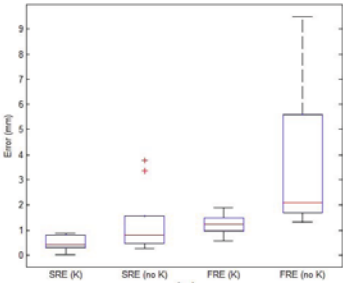

(c)

Fig. 2. Quantitative results: (a) is a summary of the quantitative phantom results comparing registration completed with and without reinforcing the point clouds with high curvature features, K. (b) is the results of the clinical data study. (c) is the box plot of the phantom results, showing the large standard deviation of the FRE in cases when curvature features are not used.

Fig. 3. Comparison of registering volumes with and without K: (a) is a slice of a CT volume. (b) is a slice of a US volume that was registered to (a) using K features. (c) is the same slice of an US volume registered without K. Notice the fiducials (red squares) are visible in (a) and (b) and not in (c), due to a misregistration along the iliac crest.

results in Figure 1 (e). The SRE was very low in all tests and averaged 0.49 mm when curvature metrics were used (vs 1.30 mm when not). The FRE noticeably improved when Gaussian curvature features, K, were used to create the point clouds, Figure 2 (c) - 1.22 vs 3.71 mm. The consistent SRE demonstrates the ability of GMM registration to reliably match surfaces; the improved FRE for tests including K indicates that curvature features improve registration when other surface features are too similar. The average run-time of the registration of all tests was less than 2.11 s. It should be noted that the PS surface has been reported to be biased slightly inwards relative to the bone surface (on the order of 0.4 mm) [9], which likely contributes slightly to the FRE.

Qualitative results of the clinical study can be seen in Figure 4. The US volumes were acquired in a region of the iliac spine unaffected by the fracture. The three pairs of registered data sets had a mean SRE of 0.63 mm and run-time of 1.99 s for tests including high curvature points and can be seen in Figure 2.

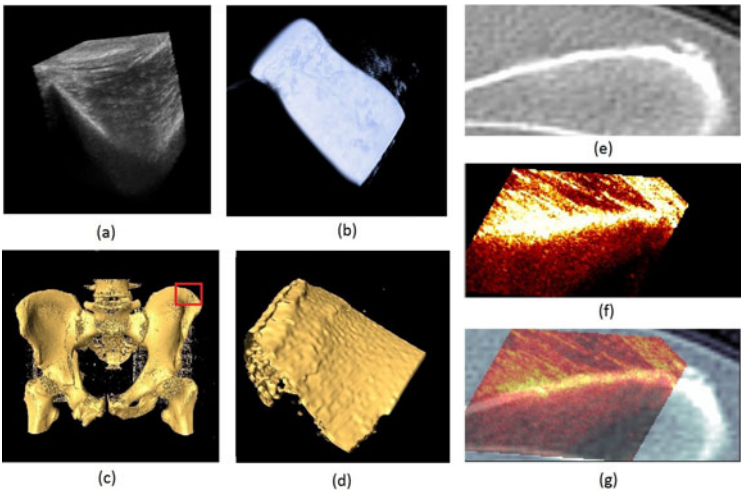

Fig. 4. Qualitative results of the clinical study: (a) is the in vivo B-Mode US and (b) is the PS. (c) is the CT data of a pelvic fracture patient with the region of interest enclosed in the red box. (d) is the thresholded region of interest. (e) and (f) are 2D slices of the CT and US respectively, and (g) is the fused overlaid slice.

4 Conclusion

We proposed a novel method for near real-time 3D US-CT registration using GMM matching of automatically extracted phase and curvature features. We demonstrated the high discriminability of our feature point extraction and have shown that reinforcing highly sub-sampled local phase information with points in high curvature regions improves the robustness and accuracy of the registration without significantly increasing the run-time of the registration. Validating our method on both phantom and real clinical data showed over 80% improvement in run-time compared to state-of-the-art methods [8] with an average accuracy improvement of over 65%. Our method is aimed for prospective US-based OR guidance and thus we will focus our future work efforts on achieving real-time operation by optimizing this algorithm to run on the GPU.

References

1. Penney, G.P., Edwards, P.J., King, A.P., Blackall, J.M., Batchelor, P.G., Hawkes, D.J.: A stochastic iterative closest point algorithm (stochastICP). In: Niessen, W.J., Viergever, M.A. (eds.) MICCAI 2001. LNCS, vol. 2208, pp. 762–769. Springer, Heidelberg (2001)
2. Barratt, D.C., Penney, G.P., Chan, C.S.K., Slomczykowski, M., Carter, T.J., Edwards, P.J., Hawkes, D.J.: Self-calibrating ultrasound-to-CT bone registration. In: Duncan, J.S., Gerig, G. (eds.) MICCAI 2005. LNCS, vol. 3749, pp. 605–612. Springer, Heidelberg (2005)

3. Moghari, M.H., Abolmaesumi, P.: Point-Based Rigid-Body Registration Using an Unscented Kalman Filter. IEEE Transactions on Medical Imaging 26(12), 1708–1728 (2007)
4. Kowal, J., Amstutz, C., Langlotz, F., Talib, H., Ballester, M.G.: Automated Bone Contour Detection in Ultrasound B-mode Images for Minimally Invasive Registration in Computer Assisted Surgery an in Vitro Evaluation. The International Journal of Medical Robotics and Computer Assisted Surgery 3(4), 341–348 (2007)
5. Winter, S., Brendel, B., Pechlivanis, I., Schmieder, K., Igel, C.: Registration of CT and Intraoperative 3-D Ultrasound Images of the Spine Using Evolutionary and Gradient-Based Methods. IEEE Transactions on Evolutionary Computation 12(3), 284–296 (2008)
6. Penney, G., Barratt, D., Chan, C., Slomczykowski, M., Carter, T., Edwards, P., Hawkes, D.: Cadaver Validation of Intensity-Based Ultrasound to CT Registration. Medical Image Analysis 10(3), 385–395 (2006)
7. Wein, W., Brunke, S., Khamene, A., Callstrom, M.R., Navab, N.: Automatic CT-ultrasound registration for diagnostic imaging and image-guided intervention. Medical Image Analysis 12(5), 577–585 (2008)
8. Gill, S., Abolmaesumi, P., Fichtinger, G., Boisvert, J., Pichora, D., Borshneck, D., Mousavi, P.: Biomechanically Constrained Groupwise Ultrasound to CT Registration of the Lumbar Spine. Medical Image Analysis (August 2010) (in press)
9. Hacihaliloglu, I., Abugharbieh, R., Hodgson, A.J., Rohling, R.: Bone segmentation and fracture detection in ultrasound using 3D local phase features. In: Metaxas, D., Axel, L., Fichtinger, G., Székely, G. (eds.) MICCAI 2008, Part I. LNCS, vol. 5241, pp. 287–295. Springer, Heidelberg (2008)
10. Gray, A.: Modern Differential Geometry of Curves and Surfaces with Mathematica, Boca Raton, FL, pp. 373–380 (1997)
11. Jian, B., Vemuri, B.: Robust Point Set Registration Using Gaussian Mixture Models. IEEE Transactions on Pattern Analysis and Machine Intelligence (2011)
12. Phillips, R.: The Accuracy of Surgical Navigation for Orthopaedic Surgery. Current Orthopaedics 21(3), 180–192 (2007)